New π^+ lifetime measurement

T. Numao, J. A. Macdonald, G. M. Marshall, and A. Olin
TRIUMF, 4004 Wesbrook Mall, Vancouver, British Columbia, Canada V6T 2A3

M. C. Fujiwara
University of British Columbia, Vancouver, British Columbia, Canada V6T 2A6
(Received 11 May 1995)

A time spectrum of surface muons from the decay $\pi^+ \to \mu^+\nu$ ($P_{\mu^+} = 30$ MeV/c) was measured using a secondary beam channel as a spectrometer, yielding the pion lifetime $\tau_\pi = 26.0231 \pm 0.0050$ (stat) ± 0.0084 (syst) ns.

PACS number(s): 13.20.Cz, 14.40.Aq

I. INTRODUCTION

Universality in the weak interactions of leptons in the three generations is one of the fundamental assumptions in the standard model. The most stringent test of e-μ universality comes from a measurement of the branching ratio of the decays $\pi^+ \to e^+\nu$ and $\pi^+ \to \mu^+\nu$ [1, 2]. The theoretical prediction for the branching ratio is $R_{\rm th} = \frac{\Gamma(\pi\to e\nu+\pi\to e\nu\gamma)}{\Gamma(\pi\to\mu\nu+\pi\to\mu\nu\gamma)} = (1.2352 \pm 0.0005) \times 10^{-4}$ [3]. The small theoretical uncertainty for this branching ratio leaves room for improvement of the experiment [presently, $R_{\rm exp} = (1.231 \pm 0.003) \times 10^{-4}$] [4,5] by almost an order of magnitude. However, the uncertainty in the pion lifetime is directly propagated to the branching ratio uncertainty [1]. The goal of a future $\pi^+ \to e^+\nu$ experiment with a 0.1% accuracy requires the present world average of the pion lifetime $\tau_\pi = 26.030 \pm 0.024$ ns [4] (0.1% contribution to the branching ratio) to be improved. Although the lifetime of the pion is not well calculated at present, the total decay rate without radiative corrections is written $\Gamma_\pi = \frac{G_F^2 f_\pi^2}{4\pi m_\pi^3} \mid V_{ud} \mid^2 \sum_{l=e,\mu} m_l^2 (m_\pi^2 - m_l^2)^2$. The pion-decay constant f_π appears in many calculations and can be taken as an important fundamental constant.

Pion lifetime measurements were often performed as a part of CPT symmetry tests. Because the measurements involved detection of both π^+ and π^-, the lifetime was determined in flight by attenuation of pion beams. The accuracy was limited by rate-dependent efficiencies and the presence of decay muons in the beam, some of which could be misidentified as pions. Ayres *et al.*, [6] found $\tau_\pi = 26.02 \pm 0.031$ (stat) ± 0.023 (syst) ns in 1971. Experiments with pions at rest were performed by several groups [7, 8]. They measured 4-MeV muons from the decay $\pi^+ \to \mu^+\nu$. Since the range of the muon is of the order of 1.5 mm, a thin target counter is required to enable efficient muon detection, resulting in a poor pion stopping rate. The measurements were therefore limited by event statistics, and the best experiment had 10^7 $\pi^+ \to \mu^+\nu$ decay events [7], which gave $\tau_\pi = 26.04 \pm 0.05$ ns. A technique was developed by a group at Leningrad [9]; they measured the time evolution of the surface-muon yield with respect to the beam burst—a surface muon [10] is a decay product of a pion, which stops near the surface of a pion production target, and the momentum spectrum has a broad peak with a very sharp upper edge at 29.8 MeV/c, corresponding to a pion decay at rest. Statistical accuracy was significantly improved by this method, but the result has not been published.

II. EXPERIMENTAL METHODS

The yield of surface muons as a function of time with respect to the beam burst was measured using a low-energy muon channel (M13) at TRIUMF [11]. This beam channel, viewing the production target at 135° with respect to the primary proton beam, had two 60° bending magnets, and was 9.4 m long to the third focus point. There were a set of jaws to limit the aperture (the largest beam envelope was limited to 3×3 cm^2 for most data taking), and two sets of slits at the first two focus points that provided a 1.0% momentum resolution [full width at half maximum (FWHM)]; these were important for reducing the pion decay contribution coming from other than the target. In order to allow a longer inspection period for pion decays, the beam burst period from the 500-MeV cyclotron (usually 43.3 ns) was increased to 216.5 ns using the 1:5 selector in the ion source. Since backgrounds above the level of 10^{-4} would contribute to systematic uncertainties, it was very important to investigate the late time region where the contribution from pion decays was reduced to tolerable background levels. Positrons in the beam were suppressed to 1/3 of the muon rate using a dc separator that added 1.5 m to the length of the secondary beam line. This extra length also provided further suppression of pions in the beam; the pion rate was less than 10^{-4} of muons at the end of the beam line. The separator, however, reduced the muon rate by a factor of 10 due to the beam optics (restricted phase space acceptance).

Muons were detected at the end of the secondary beam channel with a telescope consisting of three thin plastic scintillation counters, $B1$, $B2$, and $B3$ (0.25 mm$\times 30^\phi$ mm, 0.13 mm$\times 45^\phi$ mm, and 0.50 mm$\times 30^\phi$ mm in thickness and diameter, respectively) and a 1-cm-thick 15-cm$\times$20-cm counter $B4$ for positron detection. The first

two counters were placed about 2 cm from the end of the beam pipe. The third counter was placed 20 cm downstream of the first two counters during most runs but for some systematic tests it was placed immediately behind the two counters. The $B4$ counter was located 1 m downstream from the first counter. At the beam momentum of $P = 29.4$ MeV/c, about half the muons stopped in the third counter and all the pions in the first counter. The beam rate in the counters was 1–2 kHz.

For most runs a coincidence of the first and second counters was used as a trigger. Pulse-height and timing information was measured with analogue to digital converters (ADC's) (LeCroy 2249A and 2249W) and TDC's (LeCroy 4208 and 2228A). Signals from each counter were fed to two ADC's, one with a 30-ns gate width starting at the time of a beam particle and the other with an 800-ns width at the time of the corresponding cyclotron rf time. This allowed detection of extra particles. The timing information included the interval between the rf time and the trigger as well as the closest times of beam pile ups to the trigger. A 1-cm^3 Čerenkov counter placed in the vicinity of the production target was used to monitor the performance of the 1:5 selector. Pulses from the counter were prescaled to about 1/10 of the muon rate to form a special trigger.

The standard runs were taken at $P = 29.4$ MeV/c, which was lower by 1.5% than that of the muon from the decay $\pi^+ \rightarrow \mu^+\nu$ at rest (or the surface muon edge for the present experiment). Data were taken under various conditions to test systematic effects as well as to provide background estimations. These conditions included combinations of different production targets (12-mm-thick beryllium and 10-mm-thick carbon), counter geometries (0 and 20 cm between $B2$ and $B3$), sizes of the muon beam envelope (3 and 4 cm), and secondary-beam momenta (27.6, 29.4, 30.2, 31.1, and 60 MeV/c). Roughly $10^6 - 10^7$ muon events were recorded on tape for each run at a rate of $\sim 10^3$ s^{-1}.

The TDC (LeCroy 4208) used for the measurement of the pion decay time was calibrated using the prescaled cyclotron rf signal, which was known to the accuracy of 10^{-6}. Because the time resolution of the TDC was only 1 ns, the measurement extended up to 40 μs to provide the accurate calibration $1.000\,002\,3 \pm 0.000\,000\,1$ ns/channel.

III. ANALYSIS

A. Event selection I (background)

Pions and positrons from the production target, having a different time distribution, were the major sources of background. Pions, the range for which is 0.7 mm in scintillator at 29.8 MeV/c, barely reached the first counter after being degraded in the vacuum window of the beamline, the air and the wrapping material. They fired the $B1$ counter at 2×10^{-5} of the muon rate estimated for 29.4 MeV/c —the rate was derived by setting the beam channel momentum at 31.1 MeV/c, 4.4% higher than the surface muon peak edge, and then scaling the π/μ ratio to 29.4 MeV/c with corrections for the decay length (lower momentum) and the presence of surface muons. The fractional contribution of pions to the muon time spectrum was estimated to be 6×10^{-6} after applying the set of loose cuts described below. At this stage, the remaining "pions" were really muons that gained extra range through the decay-in-flight process near the detector.

Positrons (30% of the muon rate) originated from three sources. One was from $\pi^0 \rightarrow \gamma\gamma$ decays in the production target in which a photon converted to an e^+e^- pair; this type only had a prompt component and did not have much energy loss in the $B1$ counter. The e/μ ratio in the final spectrum was estimated to be 2×10^{-6}, and the contribution to the pion lifetime was less than 0.000 17 ns. The second type, the dominant source, was from the $\mu^+ \rightarrow e^+\nu\bar{\nu}$ decay following $\pi^+ \rightarrow \mu^+\nu$ decays in the target. This type had a "flat" time distribution and appeared to have larger energy loss in the first counter (more high-energy tail). Because positrons from this mechanism tended to come from a diffuse source around the target, they were likely to hit the surrounding annular light guide that was 20 times thicker than the scintillator itself. (In this case, the number of photons from the Čerenkov effect might have been larger than from the scintillator and resulted in a larger high-energy tail.) The third source was from old muons in the detector area that decayed back into the $B1$ counter during the inspection period. Decay positrons could hit the light guide or the scintillator. This component also had a flat-time distribution but could be suppressed by identifying the presence of earlier muons. The e/μ ratio for the two flat components was less than 6×10^{-6} and the contribution to the pion lifetime was 0.00034 ns.

The off-line version of the trigger requirement, $B1 \times B2$ coincidence with a time window of 15 ns, was good enough to suppress the pion background to a trivial level described earlier. Figure 1 shows a scatter plot of the pulse height distribution in $B1$ and $B2$. The box indicates the final cut position to suppress positrons; the cut resulted in a suppression factor of 10^{-4}. There was a definite pulse shape difference in $B1$ between positrons and muons, as shown in Fig. 2 (a scatter plot between

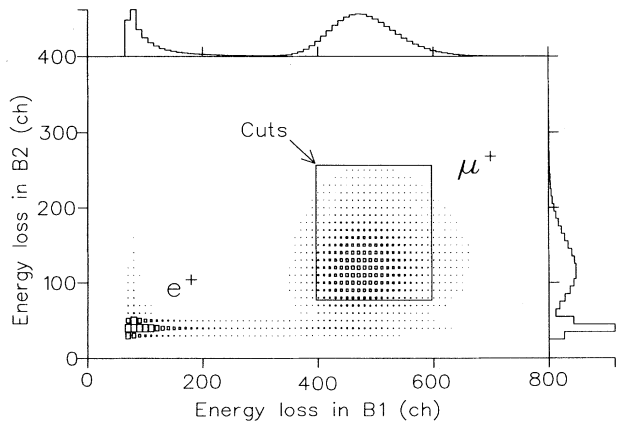

FIG. 1. Scatter plot of energies in $B1$ and $B2$. The box shows the acceptance region. These data were taken without the $B1 \times B2$ coincidence requirement.

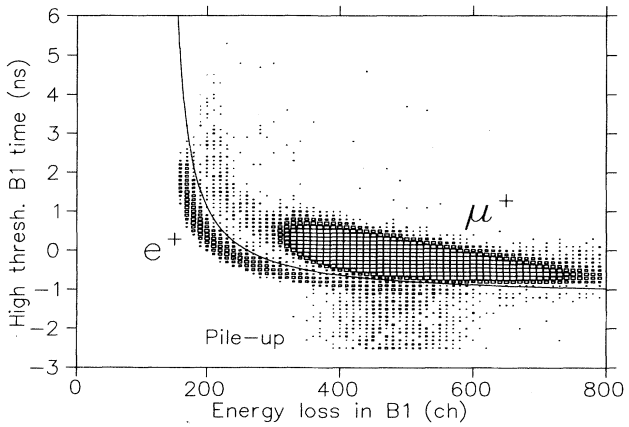

FIG. 2. Scatter plot of energy in $B1$ and "rise time" (event time at a higher threshold; the TDC's were started by the low-threshold signal). Note the majority of positrons have already been eliminated by the high threshold requirement.

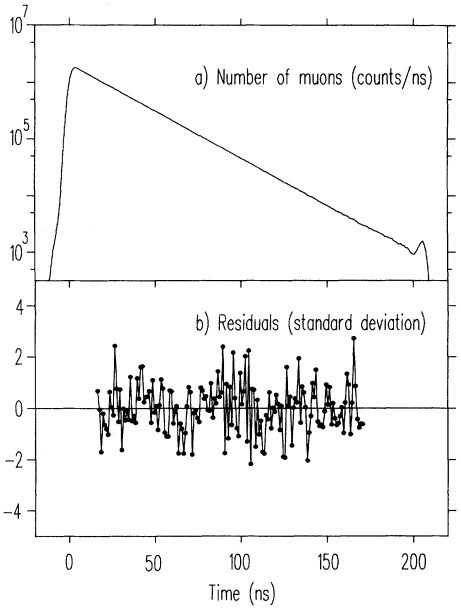

FIG. 3. (a) Time spectrum of muon yield. (b) Residuals of the fit divided by the corresponding uncertainty. This plot also indicates the fitting region.

the pulse height and the time difference at two different thresholds); a combination of the cut based on this (shown by the solid line in the figure) and one from $B2$ reduced the number of positrons by another order of magnitude.

B. Event selection II (pile up)

Events with an additional muon would lead to a shorter measured lifetime. They deposited twice the charge in the wide-gate ADC and were rejected mainly based on the high-energy-loss cut of $B1$. This rejection was augmented by the post-pile-up logic based on TDC information that was sensitive after 30 ns from the first pulse with a negligible inefficiency. The inefficiency of the pile-up detection within 30 ns of the first pulse was estimated to be about 1% from the events with a pile up in the 800-ns ADC gate period; the corresponding contribution to the pion lifetime was 0.000 05 ns. One problem associated with these pile-up cuts was that a pile up occurred in a time-dependent way, causing a time-dependent event-rejection probability; since the inspection period was determined with respect to the time of beam bursts, the time dependence of the misidentified positron from the decay of the stopping muon would cause self-vetoing and be reflected in the pile-up rejection probability. This bias, which was estimated to be 10^{-4} for the result with only the ADC pile-up information, was reduced to a level of 10^{-6} after the time window of the post-pile-up inspection period was extended to 8 μs to allow most muons to decay away.

By applying all the cuts mentioned above, possible backgrounds and distortions caused by contamination were reduced to a negligible level, and about 70% of the events were histogrammed for subsequent analysis. Figure 3(a) shows the summed time spectrum that contains 6×10^7 events.

C. Fits

The time spectra were fitted basically to a single exponential function with the decay constant and the amplitude as free parameters—additional parameters will be discussed in the following paragraphs. The time region for the standard fit was from 15 to 170 ns with respect to the beam burst (time zero). Several groups of runs were analyzed to study dependence on the muon momentum (or the pion source depth) and the target material. The final result came from the fit using the summed spectrum of ten measurements.

Because the TDC 4208 uses digital interpolation between two clock pulses (125 MHz) to achieve 1-ns resolution, there were spikes at every four and eight channels with amplitudes of ~2%. This was the major source of the bad χ^2 in the fit. The problem was solved by adding to each measured interval a random time offset up to ± 2 ns. This smoothing procedure reduced the $\sqrt{\chi^2/\mathrm{DF}}$ from 1.6 to 1.1. After the introduction of trigonometric functions with periods of 4 and 8 ns for the correction of time bin variation, a typical $\sqrt{\chi^2/\mathrm{DF}}$ further dropped to 1.0, and the 4-ns and 8-ns components were at levels of 10^{-4} and 10^{-3}, respectively, but still the lifetime did not change.

There were some indications of beam spills between the unsuppressed beam bursts coming every 216.5 ns, especially nearby the unsuppressed beam bursts (or ± 43.3 ns from time zero); there was an obvious peak corresponding to the first suppressed rf cycle in the time spectrum of the monitor Čerenkov counter, and, as shown by the open circles in Fig. 4 (the measured pion lifetimes vs the early time window edge of the fit), there was a

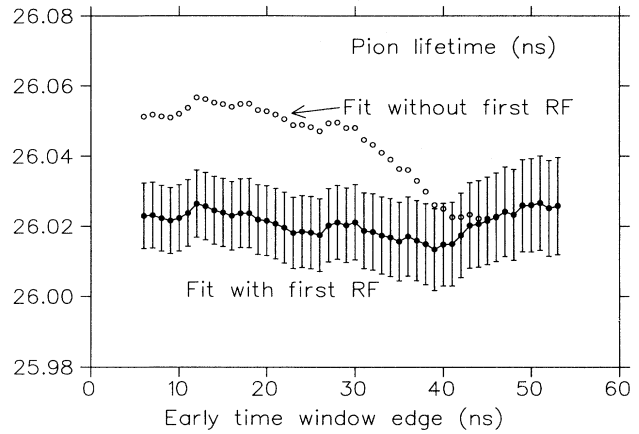

FIG. 4. Pion lifetimes as a function of the early time window edge for the fit. The closed circles indicate the fit with all the components, while the open circles indicate the fit without the first rf leakage component. The errors shown here are total errors.

small "step" around 43 ns after the time zero. These effects were more pronounced in the data taken during the tuning of the 1:5 selector. A term corresponding to the first rf-cycle leakage was introduced in the fit by shifting the observed time spectrum by 43.3 ns. The amplitude ratio of the shifted component to the unshifted was $(6.2 \pm 1.6) \times 10^{-4}$ from the monitor Čerenkov spectrum, in good agreement with $(5.7 \pm 1.6) \times 10^{-4}$ as derived from the fit of the pion decay spectrum. This correction lowered the pion lifetime by ~ 0.034 ns and contributed significantly to the final error. The leakage limits of the second and third suppressed rf cycles were also estimated to be $\leq 3.4 \times 10^{-5}$ and $\leq 3.2 \times 10^{-5}$, respectively, using the Čerenkov monitor and muon spectra from the high-momentum runs. These extra leakage limits provided additional constraints in the fit. Terms corresponding to the second and third rf-cycle leakages were also added in the fit. The time region corresponding to the fourth suppressed rf cycle, where small leakage was evident, was not included in the fit.

A cloud of slow pions drifting near the production target could produce a shorter measured lifetime, since they disappeared both by decay and by moving out of the acceptance of the measurement apparatus. In order to estimate this effect, data were taken at higher momentum $P = 30.2$ MeV/c, 1.5% above the surface muon edge. The delayed muon spectrum at this momentum provided the ratio of the effective cloud amplitude $(5.0 \pm 0.5) \times 10^{-4}$ compared to the surface muon yield and the effective lifetime of the component 22.9 ± 1.1 ns. This component was included in the fitting equation, and the above values together with the uncertainties provided external constraints to the fit. This correction increased the observed pion lifetime by 0.002 ns.

The timing resolution, which includes the effects of the beam burst shape and the time-of-flight (TOF) variation of muons, is not crucial as long as the resolution is much less than the separation between the time zero and the fitting region. The measured timing resolution for prompt muons at 31.1 MeV/c, 4.4% above the surface-muon edge, was about 1 ns (σ), and no delayed events were observed at a 10^{-4} level beyond 10 ns from the peak, except for "pions" at the corresponding TOF and sparsely distributed misidentified positrons. Therefore, timing resolution was not introduced in the fit.

The final fits included these external constraints of beam leakage and the pion cloud by adding the squares of the deviations to the χ^2, and all these components were set free. This fit yielded $\tau_\pi = 26.0231 \pm 0.0097$ ns with a $\sqrt{\chi^2/\mathrm{DF}} = 1.00$. Figure 3(b) shows the residuals of the fit normalized by the corresponding uncertainty. In order to separate the statistical error from the total error, the parameters for the pion lifetime and the surface muon yield were set free, while the rest were fixed at the values corresponding to the minimum χ^2. The statistical error obtained was 0.0050 ns. As shown by the closed circles in Fig. 4, the pion lifetime seems to be stable up to the fit including the early-time region around 5 ns from the time zero. The error bars in the figure indicate total errors. This indicates that the measured pion lifetime was not affected by the possible distortion in the early-time region.

Dependence on various cuts was studied by changing one of the parameters while keeping the others at the standard position. Variation of the energy loss cut in $B1$ did not affect the lifetime around the standard cut at channel 400. The measured lifetime started increasing as the $B1$ energy loss cut was lowered below channel 200. This was because of misidentification of positrons; without the $B1$ energy loss cut, the pion lifetime increased by 0.010 ns, and this change was consistent with the estimated positron contamination level of $10^{-4} - 10^{-3}$ without the cut. Similarly, relaxing the cuts on the energy loss in $B2$, pulse shape in $B1$, and the $B2$ timing caused no noticeable effect on the lifetime. These procedures confirmed that the positron suppression factor was adequate, and a constant term in the fit was not necessary. The measured lifetime was also tested for stability against variation of the cuts on wide-gate ADC counts as well as on the difference from the short-gate ADC's that provided additional pile-up information.

Changes in the pion population in the target by other than the decays would result in a distortion in the decay spectrum. Pion diffusion in the target was estimated to be of the order of a micron for a period of the pion lifetime, and the contribution to the lifetime measurement was less than 10^{-5}. The fraction of muons from other pion sources, such as pions stopping in the material around the target and the collimators of the secondary beam channel, was also estimated to be less than 10^{-5}. Such an effect on the pion lifetime was negligible, because the time zeros of those components were before the early-time window edge of the fit, and their major contribution to the time spectrum in the fitting region was just to increase the amplitude of the primary component.

IV. RESULTS

Major sources of systematic uncertainties discussed above are listed in Table I. All systematic uncertainties

TABLE I. Systematic uncertainties.

Sources	Uncertainties (ns)
Beam leakage,[a] slow π[a]	0.0083
Prompt positron background	0.0002
Flat positron background	0.0003
Pion background	0.0002
Extra muons	0.0001
Other pion sources	0.0001
Diffusion	0.0003
Total uncertainty	0.0084

[a]Included in the fit.

TABLE II. Lifetimes for different conditions.

Conditions	Lifetime (ns)	Tests
Final result	26.0231±0.0097	
$B1B2B3$	26.0210±0.0117	Positrons
Free flat background	26.0260±0.0113	Positrons, other
$P = 27.6$ MeV/c	26.0288±0.0186	Positrons, π cloud
$P = 29.4$ MeV/c	26.0196±0.0101	Diffusion
C target	26.0198±0.0107	π^+ diffusion
Be target	26.0260±0.0129	
Slit 3 cm	26.0226±0.0169	π cloud
Slit 4 cm	26.0239±0.0104	

were combined quadratically. The final result of our measurement is 26.0231 ± 0.0050 (stat) ± 0.0084 (syst) ns. This is consistent with the world average, 26.030 ± 0.024 ns [4].

In order to further confirm the above estimations and nonexistence of unexpected effects, the amplitude for the additional flat-background component was set free in the fit. The result is consistent with the standard fit and is shown in Table II. It also shows results of analyses of different experimental conditions, i.e., requiring $B3$ in the event definition, beam channel momenta, stopping counter positions, production targets, and slit settings. The uncertainties are a sum of statistical and systematical errors. All the results are consistent, confirming the error estimations in Table I.

Note added. After submission of our paper, V.P. Koptev *et al.* published a new pion lifetime: $\tau = 26.0361 \pm 0.0052$ ns; see Ref. [12].

ACKNOWLEDGMENTS

The authors wish to thank Dr. D.A. Bryman for valuable discussions and comments and Dr. J. Doornbos for the beam transport calculations.

[1] D.I. Britton *et al.*, Phys. Rev. Lett. **68**, 3000 (1992); Phys. Rev. D **49**, 28 (1994).
[2] G. Czapek *et al.*, Phys. Rev. Lett. **70**, 17 (1993).
[3] W.J. Marciano and A. Sirlin, Phys. Rev. Lett. **71**, 3629 (1993).
[4] Particle Data Group, L. Montanet *et al.*, Phys. Rev. D **50**, 1173 (1994).
[5] T. Numao, Mod. Phys. Lett. A **7**, 3357 (1992); D.A. Bryman, Comments Nucl. Part. Phys. **21**, 101 (1993).
[6] D.S. Ayres *et al.*, Phys. Rev. D **3**, 1051 (1971).
[7] M.E. Nordberg *et al.*, Phys. Lett. **24B**, 594 (1967).
[8] A.F. Dunaitsev *et al.*, Sov. J. Nucl. Phys. **16**, 292 (1973).
[9] N.K. Abrosimov *et al.*, Report No. Leningrad-85-1073, 1985 (in Russian) (unpublished), see *Note added.*
[10] A.E. Pifer, T. Brown, and K.R. Kendall, Nucl. Instrum. Methods **135**, 39 (1976).
[11] C.J. Oram *et al.*, Nucl. Instrum. Methods **179**, 95 (1981).
[12] V.P. Koptev *et al.*, JETP Lett. **61**, 877 (1995).